NONLINEAR ANALYSIS OF STABILITY FOR IMPERFECT ECCENTRICALLY STIFFENED FGM PLATES UNDER MECHANICAL AND THERMAL LOADS BASED ON FSDT. PART 2: NUMERICAL RESULTS AND DISCUSSIONS

Dao Van Dung, Nguyen Thi Nga*
VNU University of Science, Hanoi, Vietnam
*E-mail: nguyennga282@gmail.com
Received February 02, 2015

Abstract. Based on the first-order shear deformation plate theory (FSDT), the smeared stiffeners technique and Galerkin method, the analytical expressions to determine the static critical buckling load and analyze the post-buckling load-deflection curves of FGM plates reinforced by FGM stiffeners resting on elastic foundations and subjected to in-plane compressive loads or thermal loads are established in part 1. In this part, we will use them to study the effects of temperature, stiffener, volume fraction index, geometrical parameters, elastic foundations on the buckling and post-buckling behavior of plates. In addition, the results in comparisons between the classical plate theory (CPT) and the first order shear deformation theory (FSDT) also are carried out and shown that the buckling and post-buckling behavior of more thick plate should be studied by FSDT.

Keywords: Stiffened plates, nonlinear analysis, functionally graded material (FGM), thermal environment, elastic foundation, analytical approach.

1. INTRODUCTION

Governing equations of this problem are established in part 1: "Nonlinear analysis of stability for imperfect eccentrically stiffened FGM plates under mechanical and thermal loads based on FSDT. Part 1: Governing equations establishment" of the paper. In this part, the effect of temperature, stiffener, volume fraction index, geometrical parameters, elastic foundations on the buckling response of plates are numerically investigated.

Analytical approach have become popular to investigate nonlinear static response of mechanic structure analysis. Tung and Duc [1] used an analytical approach to investigate the stability of functionally graded un-stiffened plates under mechanical and thermal loads. Dung and Hoa [2] presented an analytical study of nonlinear static buckling and post-buckling analysis of eccentrically stiffened functionally graded circular cylindrical shells under external pressure. Kiani and Eslami [3] studied analytically the buckling

of heated functionally graded material annular plates on Pasternak-type elastic foundation based on the CPT. Naderi et al. [4] presented an exact analytical solution for buckling analysis of moderately thick functionally graded sector plates resting on Winkler elastic foundation according to FSDT.

Many researches take into account the contribution of stiffeners by the smeared stiffeners technique, such as [2,5,6]. Bich et al. [5] investigated nonlinear dynamical analysis of eccentrically stiffened functionally graded cylindrical panels. Nonlinear dynamic analysis of eccentrically stiffened functionally graded circular cylindrical thin shells surrounded by an elastic medium are presented Dung and Nam [6].

The obtained equations in part 1 [7] are used in numerical results as: Eqs. (38), (40) for FGM plates reinforced by FGM stiffeners subjected to mechanical compressive loads, Eqs. (49), (50) for FGM plates reinforced by FGM stiffeners subjected to uniform temperature rise, Eq. (54) for FGM plates reinforced by homogeneous stiffeners subjected to nonlinear temperature change and Eq. (57) for FGM plates reinforced by FGM stiffeners subjected to the combined mechanical and thermal loads. Numerical results are presented to illustrate the effects of various parameters such as temperature, stiffener, volume fraction index of material and foundation stiffness on the nonlinear stability of stiffened FGM plates. The comparison between CPT and FSDT also is carried out. The present results show that if the buckling and post-buckling behavior of more thick plate should be studied by FSDT, it will obtain the more suitable results.

2. NUMERICAL RESULTS AND DISCUSSIONS

2.1. Comparison results

As part of the validation of the present approach, firstly, a simply supported un-stiffened isotropic square plate under uniaxial compressive load without elastic foundations is considered. The geometrical and material properties of plate are taken by [8] $a = b = 10$ in, $h = 0.1$ in, $E = 3.0 \times 10^6$ psi, $v = 0.316, k = 0, \lambda = 0$. The buckling load parameter $\overline{N}_x = \dfrac{-P_x h a^2}{D_o}$, in which $D_0 = \dfrac{Eh^3}{12(1-v^2)}$ and P_x are given by Eq. (40) in part 1. The present results are compared with the results of Timoshenko and Gere [9] in Tab. 1.

Table 1. Comparison with the results of Timoshenko and Gere [9] for un-stiffened isotropic plates without elastic foundations

Mode (m, n)	Present	Timoshenko and Gere [9]
(1, 1)	39.4556	39.476
(2, 1)	61.5961	61.681
(3, 1)	109.3467	109.66
(2, 2)	157.5499	157.90

As can be seen that the obtained results are very in good agreement to those [9] based on CPT for the thin plate.

The second comparison is carried out for the following material properties and geometrical parameters of un-stiffened FGM plates [10] $E_m = 70$ GPa, $E_c = 380$ GPa, $\nu = 0.3, h = 0.005, b/h = 100, \lambda = 1, m = n = 1$. The buckling load parameter in [10] $P^* = bhP_x$ (kN) where P_x is calculated by Eq. (40) in part 1, $b/a = 1; 2, k = 0; 1; 5; 10$. The results are compared with those of Mozafari and Ayob [10] in Tab. 2.

Table 2. Comparison with the results of Mozafari and Ayob [10] for un-stiffened FGM plates without elastic foundations

		Present	CPT [10]	FSDT [10]
$\dfrac{b}{a} = 1$	$k = 0$	171.627	171.724	170.012
	$k = 1$	85.554	85.594	84.721
	$k = 5$	56.450	56.483	55.801
	$k = 10$	51.414	51.443	50.615
$\dfrac{b}{a} = 2$	$k = 0$	428.705	429.310	423.754
	$k = 1$	213.732	213.985	210.904
	$k = 5$	141.003	141.208	138.905
	$k = 10$	128.410	128.620	125.918

As can be seen that the present results in Tab. 2 are very close to those [10] based on CPT. It is correct because the considered plate is thin. However the present results are different with those of [10] calculated by FSDT because the critical buckling load of this case is the critical value of $P_{x\ upper}$.
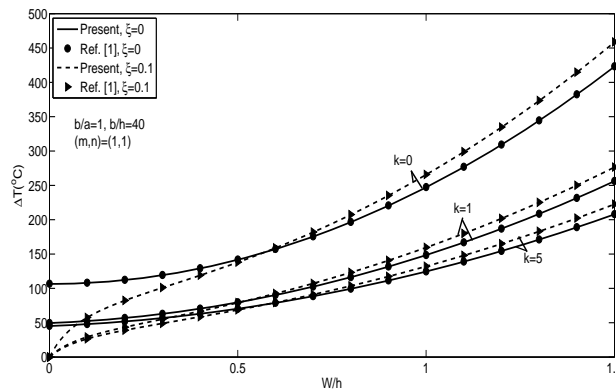

Fig. 1. Comparison with the results [1] for un-stiffened FGM plates without elastic foundations and under the uniform temperature rise

Finally, a FGM plate consisting of alumina and aluminum is considered. Young's modulus, the thermal expansion coefficient, and the conductivity coefficient for alumina are $E_c = 380 \times 10^9$ Pa, $\alpha_c = 7.4 \times 10^{-6}$ °C^{-1}, $K_c = 10.4$ W/mK, and for aluminum are $E_m = 70$ Pa, $\alpha_m = 23 \times 10^{-6}$ °C^{-1}, $K_m = 204$ W/mK, respectively. Poisson's ratio is chosen to be $\nu = 0.3$. The obtained numerical results based on FSDT for un-stiffened FGM

plates without elastic foundations and under the uniform temperature rise are compared with the results of Tung and Duc [1] based on the CPT (Fig. 1). It is seen that the comparison results in this case are in good agreement to those of [1].

2.2. Numerical results for ES-FGM plates on elastic foundations

In this section the formulations in part 1 are used to analyze the effects of input parameters on buckling and post-buckling behavior of plates. The geometric properties of the ES-FGM plate are $b = 0.8$ m, $h = 0.02$ m, $h_1 = h_2 = 0.01$ m, $b_1 = b_2 = 0.005$ m, $d_1 = d_2 = 0.08$ m. The combination of materials is the same with the last comparison of previous section. The elastic foundation parameters are used as $K_1 = 2.5 \times 10^8$ N/m^3, $K_2 = 5 \times 10^5$ N/m.

2.2.1. *Effect of temperature on post-buckling load-deflection curves of orthogonally stiffened FGM plates*

Fig. 2 shows effects of temperature rise on post-buckling behavior of ES-FGM square plates under mechanical compression load on elastic foundations. When the temperature takes the values $\Delta T = 0, 200°$C, $300°$C, and $a/b = 1, k = k_2 = k_3 = 1, (m, n) = (1, 1)$, it can be seen that the post-buckling curves become to be lower gradually with increase of ΔT. This is reasonable because the preheated ES-FGM plates exhibit a decreasing tendency in post-buckling loading carrying capacity when they are subjected to added action of mechanical loads.
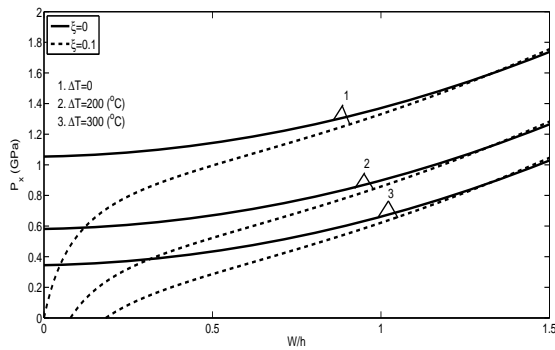

Fig. 2. Effects of temperature rise on post-buckling behavior of FGM plates reinforced by FGM stiffeners on elastic foundations under uniaxial compression
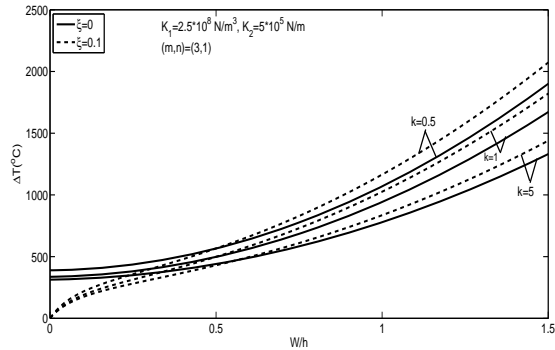
Fig. 3. Post-buckling curves of FGM plates reinforced by FGM stiffeners on elastic foundations under uniform temperature rise with k

2.2.2. *Effect of volume fraction index k on post-buckling curves $\Delta T - W/h$*

This section shows the effects of the volume fraction index k on post-buckling curves $\Delta T - W/h$ of ES-FGM square plates with $k = 0.5; 1; 5$ and $\xi = 0; \xi = 0.1$, and $(m, n) = (3, 1)$.

Figs. 3 and 4 show the effects of k on the post-buckling curves of orthogonally stiffened FGM plates on elastic foundations and without foundations under uniform temperature rise.
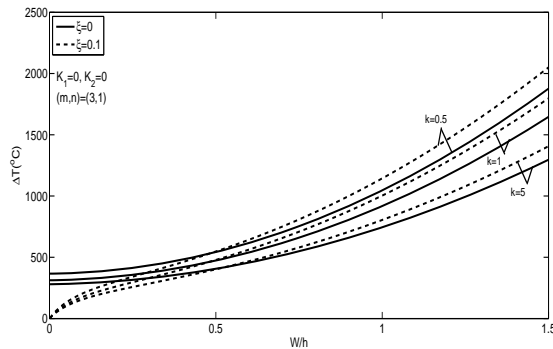
Fig. 4. Post-buckling curves of FGM plates reinforced by FGM stiffeners without foundations under uniform temperature rise with k
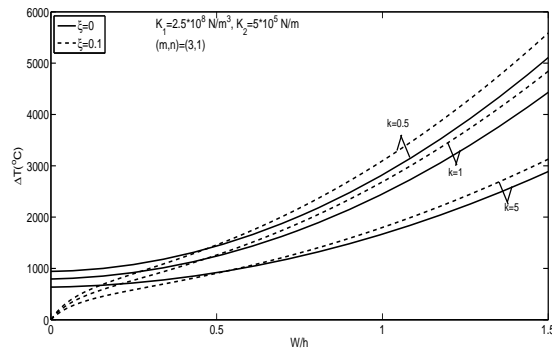
Fig. 5. Post-buckling curves of ES-FGM plates on elastic foundations under nonlinear temperature change with k

Fig. 5 shows the effects of k on the post-buckling curves of ES-FGM plates resting on elastic foundations under nonlinear temperature change.

It can be seen from all figures that the post-buckling load-deflection curves become lower when the values of k increase.

2.2.3. *Comparison of the critical buckling load between a plate with FGM stiffener and homogeneous stiffener*

Tab. 3 compares the critical buckling load of an orthogonally stiffened FGM square plate under biaxial compression ($\lambda = 1; 2$) with $k = 0.5; 1; 2; 5$ and 10. It can be seen that the critical buckling loads of FGM plate reinforced FGM stiffeners are larger than those of FGM plates reinforced homogeneous stiffeners with the same value of k.

Table 3. Critical upper buckling loads for an orthogonally stiffened FGM plate under biaxial compression ($k_2 = k_3 = k$)

λ	k	P_{xcr}(GPa)	
		Homogeneous stiffeners	FGM stiffeners
	$k = 0.5$	0.7171 $(1, 1)^a$	0.7475 $(1, 1)$
	$k = 1$	0.6539 $(1, 1)$	0.6806 $(1, 1)$
$\lambda = 1$	$k = 2$	0.6078 $(1, 1)$	0.6284 $(1, 1)$
	$k = 5$	0.5740 $(1, 2)$	0.5934 $(1, 1)$
	$k = 10$	0.5398 $(1, 2)$	0.5600 $(1, 2)$
	$k = 0.5$	0.4781 $(1, 1)$	0.4984 $(1, 1)$
	$k = 1$	0.4181 $(1, 2)$	0.4537 $(1, 1)$
$\lambda = 2$	$k = 2$	0.3548 $(1, 2)$	0.3926 $(1, 2)$
	$k = 5$	0.3189 $(1, 2)$	0.3397 $(1, 2)$
	$k = 10$	0.2999 $(1, 2)$	0.3111 $(1, 2)$

^{a} Buckling mode (m, n).

2.2.4. *Effect of stiffeners on the critical upper buckling load of FGM plates without foundations*

Tabs. 4 and 5 present the results of the critical buckling load of FGM plates in four cases as follows: without stiffeners, transversal stiffeners, longitudinal stiffeners, orthogonal stiffeners. From Tab. 4, it can be seen that the critical buckling load of plate only attached by x-stiffener or by y-stiffener has the same value. This is correct because the plate is square whereas the value of these types of stiffeners has the differences for rectangular plates in Tab. 5. The combination of longitudinal and transversal stiffeners has strongly effect on the stability of plate. The critical load in this case is biggest. For example, with $\lambda = 1$, $P_{xcr} = 0.2503$ (GPa) for orthogonal stiffener of the square plate, $P_{xcr} = 0.1646$ (GPa) for orthogonal stiffener of the rectangular plate. In addition, the critical load of the plate subjected to uniaxial compression is bigger than one of plate subjected to biaxial compression, for example with the orthogonally stiffened rectangular plate, $P_{xcr} = 0.5005$ (GPa) for $\lambda = 0$ and $P_{xcr} = 0.1646$ (GPa) for $\lambda = 1$. As results in Tabs. 4 and 5, it can be seen that the critical buckling load of stiffened plate is greater than that of un-stiffened plate. It is reasonable because the present of stiffeners make the plate to become more rigid.

Table 4. Critical compressive load for different types of stiffeners of square plates
$(a/b = 1, k_2 = k_3 = k = 1)$

	P_{xcr} (GPa)			
	$\lambda = 0$	$\lambda = 1$	$\lambda = 2$	$\lambda = 3$
Without stiffeners	0.4267 (1, 1)	0.2134 (1, 1)	0.1422 (1, 1)	0.1067 (1, 1)
Transversal stiffeners	0.4632 (1, 1)	0.2316 (1, 1)	0.1544 (1, 1)	0.1158 (1, 1)
Longitudinal stiffeners	0.4632 (1, 1)	0.2316 (1, 1)	0.1544 (1, 1)	0.1158 (1, 1)
Orthogonal stiffeners	0.5005 (1, 1)	0.2503 (1, 1)	0.1668 (1, 1)	0.1251 (1, 1)

Table 5. Critical compressive load for different types of stiffeners of rectangular plates
$(a/b = 2, k_2 = k_3 = k = 1)$

	P_{xcr} (GPa)			
	$\lambda = 0$	$\lambda = 1$	$\lambda = 2$	$\lambda = 3$
Without stiffeners	0.4267 (2, 1)	0.1335 (1, 1)	0.0742 (1, 1)	0.0513 (1, 1)
Transversal stiffeners	0.4632 (2, 1)	0.1626 (1, 1)	0.0903 (1, 1)	0.0625 (1, 1)
Longitudinal stiffeners	0.4632 (2, 1)	0.1353 (1, 1)	0.0752 (1, 1)	0.0521 (1, 1)
Orthogonal stiffeners	0.5005 (2, 1)	0.1646 (1, 1)	0.0914 (1, 1)	0.0633 (1, 1)

2.2.5. *Effect of elastic foundations on un-stiffened FGM plates*

Tab. 6 shows the effects of elastic foundations on the critical compressive load of un-stiffened FGM plate by using Eq. (40) in part 1 with $q = 0$, $a = b = 0.8$ m, $k = 1$.

Tab. 7 shows the effects of elastic foundations on the critical thermal load of unstiffened FGM plate by using Eq. (50) in part 1.

As can be observed that the critical buckling load corresponding to both two parameters of foundation $K_1 \neq 0, K_2 \neq 0$ is the biggest, but if $K_1 = 0, K_2 \neq 0$ then the critical load is the smallest. In addition, the value of P_{xcr} decreases when the value of λ increases.

Table 6. Effects of elastic foundations on the critical compressive load

K_1 (N/m^3), K_2 (N/m)	P_{xcr} (GPa)			
	$\lambda = 0$	$\lambda = 1$	$\lambda = 2$	$\lambda = 3$
$K_1 = 2.5 \times 10^8$; $K_2 = 5 \times 10^5$	0.8977 (2, 1)	0.6436 (1, 1)	0.3990 (1, 2)	0.2762 (1, 2)
$K_1 = 2.5 \times 10^8$; $K_2 = 0$	0.8664 (2, 1)	0.6186 (1, 1)	0.3851 (1, 2)	0.2666 (1, 2)
$K_1 = 0$; $K_2 = 5 \times 10^5$	0.4767 (1, 1)	0.2384 (1, 1)	0.1589 (1, 1)	0.1192 (1, 1)

Table 7. Effects of elastic foundations on the critical thermal load for FGM plates subjected uniform temperature rise

K_1 (N/m^3), K_2 (N/m)	$\Delta T_{cr}(m, n)(^\circ\text{C})$		
	$k = 0.5$	$k = 2$	$k = 5$
$K_1 = 2.5 \times 10^8$; $K_2 = 5 \times 10^5$	153.9776 (1, 1)	157.3105 (1, 1)	172.6819 (2, 1)
$K_1 = 2.5 \times 10^8$; $K_2 = 0$	148.5383 (1, 1)	150.7203 (1, 1)	164.6422 (2, 1)
$K_1 = 0$; $K_2 = 5 \times 10^5$	65.7992 (1, 1)	50.4745 (1, 1)	53.2866 (1, 1)

2.2.6. *Effect of stiffeners and elastic foundations*

Tab. 8 shows the effects of stiffeners and elastic foundations on the critical compressive load of orthogonally stiffened FGM square plates. As can be seen that the critical buckling load corresponding to two-parameter foundations is the biggest and the one corresponding to only the coefficient K_2 is the smallest. In addition, the critical compressive loads of plate having both stiffeners and foundations are larger than the ones only having the foundations without the stiffeners. For example, $k = 1$, $\lambda = 0$, the value of P_{xcr} is 1.0513 (GPa) (in Tab. 8) and the value of P_{xcr} is 0.8977 (GPa) (in Tab. 6) with FGM plates on the Pasternak foundation.

Fig. 6 shows the effect of foundations on post-buckling curves $\Delta T - W/h$ of FGM plates reinforced by orthogonal FGM stiffeners subjected to the uniform temperature rise.

Fig. 7 shows the effect of foundations on post-buckling curves $\Delta T - W/h$ of orthogonal stiffened FGM plates subjected to the nonlinear temperature change.

As can be observed that the post-buckling curve $\Delta T - W/h$ of plate resting on the Pasternak foundation is highest i.e. the load carrying capacity in the case is the best but the one on the Winkler foundation is lower and the one without foundation is lowest. In addition, the increasing of the value of ΔT leads to the increasing of the deflection.

Table 8. Effect of stiffeners and foundations on the critical compress load (GPa) ($k_2 = k_3 = k$)

| K_1 (N/m^3); K_2 (N/m)	P_{xcr} (GPa) (m, n)				
	$k = 0.5$	$k = 1$	$k = 2$	$k = 5$	$k = 10$
$\lambda = 0$					
$K_1 = 2.5 \times 10^8$; $K_2 = 5 \times 10^5$	1.2626 (2, 1)	1.0513 (2, 1)	0.8834 (2, 1)	0.7644 (2, 1)	0.7001 (2, 1)
$K_1 = 2.5 \times 10^8$; $K_2 = 0$	1.2313 (2, 1)	1.0201 (2, 1)	0.8522 (2, 1)	0.7332 (2, 1)	0.6688 (2, 1)
$K_1 = 0$; $K_2 = 5 \times 10^5$	0.6845 (1, 1)	0.5505 (1, 1)	0.4462 (1, 1)	0.3763 (1, 1)	0.3391 (1, 1)
$\lambda = 1$					
$K_1 = 2.5 \times 10^8$; $K_2 = 5 \times 10^5$	0.7475 (1, 1)	0.6806 (1, 1)	0.6284 (1, 1)	0.5934 (1, 1)	0.5600 (2, 1)
$K_1 = 2.5 \times 10^8$; $K_2 = 0$	0.7225 (1, 1)	0.6556 (1, 1)	0.6034 (1, 1)	0.5684 (1, 1)	0.5350 (2, 1)
$K_1 = 0$; $K_2 = 5 \times 10^5$	0.3423 (1, 1)	0.2753 (1, 1)	0.2231 (1, 1)	0.1881 (1, 1)	0.1695 (1, 1)
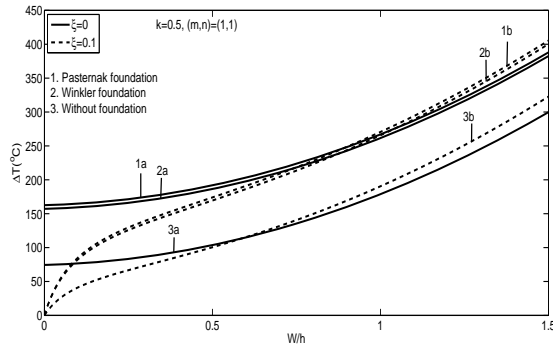
Fig. 6. The effect of foundations on FGM plates reinforced by FGM stiffeners subjected uniform temperature rise
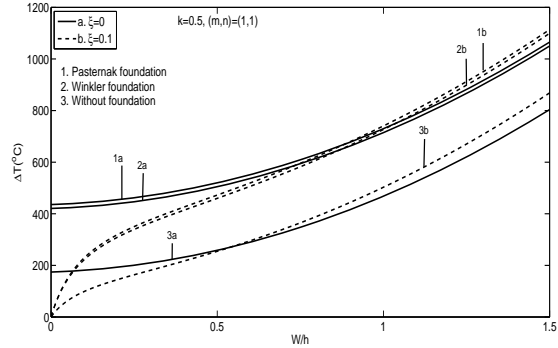

Fig. 7. The effect of foundations on ES-FGM plates subjected nonlinear temperature change

2.2.7. *Effect of imperfection*

Figs. 8 and 9 show the effect of initial imperfection on post-buckling behavior of plates with $\xi =$ 0; 0.1; 0.2; 0.3. It is observed that the post-buckling loading capacity of plates is reduced with the increase of imperfection size ξ when the deflection is still small, but an inverse trend occurs when the deflection is sufficiently large.
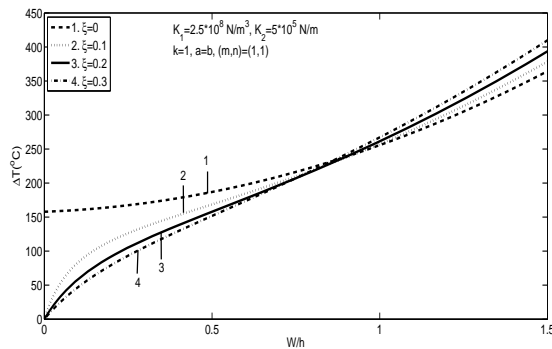
Fig. 8. Post-buckling curves of FGM plates reinforced by FGM stiffeners on elastic foundations under uniform temperature rise with ξ
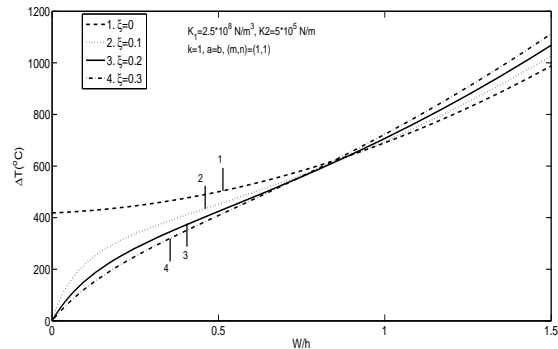
Fig. 9. Post-buckling curves of ES-FGM plates on elastic foundations under nonlinear temperature change with ξ

2.2.8. *Comparisons between CPT and FSDT*

– *First comparison:*

Tab. 9 presents the comparison between CPT with FSDT by using the above given database and Eqs. (40), (41) in part 1. Consider the ratio a/h varies from 10 to 150. It is seen that the value of the critical compressive load P_{xcr}^{CPT} and P_{xcr}^{FSDT} are close to each other for thin plates. However for more thick plates, the difference between two these theories is considerable. For example, with $a/h = 10$, the value of $P_{xcr}^{FSDT} = 38.4143$ GPa is different to $P_{xcr}^{CPT} = 42.9885$ GPa about 10.64%. This remark was noted by [11] for un-stiffened FGM rectangular plates without elastic foundations.

Table 9. Comparison the critical buckling load P_{xcr} (GPa) between FSDT (present) and CPT [5] ($a/b = 2$, $k = 1$, $\lambda = 0$, $m = n = 1$)

a/h	P_{xcr}^{FSDT} (FGM stiffeners, $k_2 = k_3 = k$)	P_{xcr}^{FSDT} (homogeneous stiffeners)	P_{xcr}^{CPT} [5]
10	38.7732	38.4143	42.9885
20	10.7244	10.4910	10.8046
30	4.9479	4.7685	4.8322
40	2.8687	2.7174	2.7379
50	1.8931	1.7583	1.7669
60	1.3585	1.2344	1.2386
70	1.0342	0.9174	0.9197
80	0.8229	0.7111	0.7124
90	0.6777	0.5694	0.5703
100	0.5737	0.4679	0.4685
120	0.4384	0.3357	0.3360
150	0.3290	0.2277	0.2278

Tab. 9 also shows that the values of the critical compressive loads P_{xcr}^{FSDT} for FGM stiffeners are larger than those for homogeneous stiffeners.

– Second comparison:

Consider a plate with the input parameters as following $E_c = 80 \times 10^9$ Pa, $\alpha_c = 7.4 \times 10^{-6}\,°C^{-1}$, $K_c = 10.4$ W/mK, $E_m = 70$ Pa, $\alpha_m = 23 \times 10^{-6}\,°C^{-1}$, $K_m = 204$ W/mK, $\nu = 0.3, b/a = 1, k = 0.5, (m, n) = (1, 1)$.

Tab. 10 compares the effects of temperature rise on post-buckling behavior of FGM plates under uniaxial compressive load calculated by CPT [1] and FSDT (present) for thin plate $(b/h = 30)$.

Table 10. Comparison of effects of temperature rise on post-buckling behavior of FGM plates under uniaxial compression calculated by CPT [1] and FSDT (present), $b/h = 30$

(a) Perfect plates

$\xi = 0$		P_x(GPa)				
W/h		0.3	0.6	0.9	1.2	1.5
$\Delta T = 0°C$	CPT [1]	0.8349	1.0136	1.2973	1.6861	2.1799
	FSDT (Present)	0.8305	1.0091	1.2928	1.6814	2.1751
$\Delta T = 100°C$	CPT [1]	0.5874	0.7661	1.0499	1.4386	1.9324
	FSDT (Present)	0.5830	0.7616	1.0453	1.4339	1.9276
$\Delta T = 200°C$	CPT [1]	0.3399	0.5186	0.8024	1.1911	1.6849
	FSDT (Present)	0.3355	0.5142	0.7978	1.1865	1.6801

(b) Imperfect plates

$\xi = 0.1$		P_x(GPa)				
W/h		0.3	0.6	0.9	1.2	1.5
$\Delta T = 0°C$	CPT [1]	0.6796	0.9749	1.3263	1.7676	2.3074
	FSDT (Present)	0.6763	0.9710	1.3221	1.7632	2.3028
$\Delta T = 100°C$	CPT [1]	0.4321	0.7274	1.0788	1.5201	2.0599
	FSDT (Present)	0.4288	0.7235	1.0746	1.5157	2.0554
$\Delta T = 200°C$	CPT [1]	0.1846	0.4799	0.8313	1.2726	1.8124
	FSDT (Present)	0.1813	0.4760	0.8271	1.2683	1.8079

Tab. 11 compares the effects of temperature rise on post-buckling behavior of FGM plates under uniaxial compressive load calculated by CPT [1] and FSDT (present) for more thick plate $(b/h = 10)$.

As can be seen that, from Tabs. 10 and 11, the value of the compressive load P_x of CPT and FSDT are close to each other for thin plate (with the ratio $b/h = 30$). However for more thick stiffened plates $(b/h = 10)$ the differences between the theories are more considerable. For example, with $b/h = 10, \Delta T = 100°C, \xi = 0.1, W/h = 0.3$, the value

Table 11. Comparison of effects of temperature rise on post-buckling behavior of FGM plates under uniaxial compression calculated by CPT [1] and FSDT (present), $b/h = 10$

(a) Perfect plates

$\xi = 0$		P_x(GPa)				
W/h		0.3	0.6	0.9	1.2	1.5
$\Delta T = 0°C$	CPT [1]	7.5137	9.1223	11.6761	15.1751	19.6193
	FSDT (Present)	7.1771	8.7765	11.3212	14.8111	19.2461
$\Delta T = 100°C$	CPT [1]	7.2663	8.8748	11.4286	14.9276	19.3718
	FSDT (Present)	6.9296	8.5291	11.0737	14.5636	18.9986
$\Delta T = 200°C$	CPT [1]	7.0188	8.6273	11.1811	14.6801	19.1243
	FSDT (Present)	6.6821	8.2816	10.8262	14.3161	18.7512

(b) Imperfect plates

$\xi = 0.1$		P_x(GPa)				
W/h		0.3	0.6	0.9	1.2	1.5
$\Delta T = 0°C$	CPT [1]	6.1162	8.7738	11.9363	15.9084	20.7665
	FSDT (Present)	5.8614	8.4748	11.6141	15.5696	20.4138
$\Delta T = 100°C$	CPT [1]	5.8687	8.5263	11.6888	15.6609	20.5190
	FSDT (Present)	5.6140	8.2274	11.3666	15.3221	20.1663
$\Delta T = 200°C$	CPT [1]	5.6212	8.2789	11.4413	15.4134	20.2715
	FSDT (Present)	5.3665	7.9799	11.1191	15.0746	19.9188

of $P_x = 5.6140$ GPa (FSDT) is different to $P_x = 5.8687$ GPa (CPT) about 4.34%. This result once again affirms that the use of FSDT to investigate the buckling and post-buckling behavior for thick plate is more suitable.

3. CONCLUSIONS

Using the closed-form expressions for determine the buckling load and post-buckling load-deflection curves obtained in part 1, the effects of temperature, stiffener, material properties, geometrical parameters and foundation parameters are analyzed in detail. Some remarks are deduced from present results as:

i) The values of the critical mechanical buckling load calculated by CPT and by FSDT are close to each other for thin plate. However for more thick plates, the differences between two these theories are more considerable. The critical buckling load and post-buckling behavior of more thick plate should be studied by FSDT.

ii) The FGM plate reinforced FGM stiffeners work better than the FGM plate reinforced homogeneous stiffeners.

iii) The thermal element, stiffener, foundation parameters and volume index affect strongly buckling and post-buckling behavior of plates.

ACKNOWLEDGEMENT

REFERENCES

[1] H. V. Tung and N. D. Duc. Nonlinear analysis of stability for functionally graded plates under mechanical and thermal loads. *Composite Structures*, **92**, (5), (2010), pp. 1184–1191.

[2] D. V. Dung and L. K. Hoa. Nonlinear buckling and post-buckling analysis of eccentrically stiffened functionally graded circular cylindrical shells under external pressure. *Thin-Walled Structures*, **63**, (2013), pp. 117–124.

[3] Y. Kiani and M. R. Eslami. An exact solution for thermal buckling of annular FGM plates on an elastic medium. *Composites Part B: Engineering*, **45**, (1), (2013), pp. 101–110.

[4] A. Naderi and A. R. Saidi. Exact solution for stability analysis of moderately thick functionally graded sector plates on elastic foundation. *Composite Structures*, **93**, (2), (2011), pp. 629–638.

[5] D. H. Bich, D. V. Dung, and V. H. Nam. Nonlinear dynamical analysis of eccentrically stiffened functionally graded cylindrical panels. *Composite Structures*, **94**, (8), (2012), pp. 2465–2473.

[6] D. V. Dung and V. H. Nam. Nonlinear dynamic analysis of eccentrically stiffened functionally graded circular cylindrical thin shells under external pressure and surrounded by an elastic medium. *European Journal of Mechanics-A/Solids*, **46**, (2014), pp. 42–53.

[7] D. V. Dung and N. T. Nga. Nonlinear analysis of stability for imperfect eccentrically stiffened FGM plates under mechanical and thermal loads based on FSDT. Part 1: Governing equations establishment. *Vietnam Journal of Mechanics*, **37**, (3), (2015), pp. 187–204.

[8] X. Zhao, Y. Lee, and K. M. Liew. Mechanical and thermal buckling analysis of functionally graded plates. *Composite Structures*, **90**, (2), (2009), pp. 161–171.

[9] S. P. Timoshenko and J. M. Gere. *Theory of elastic stability*. Mc Graw-Hill, New York, (1961).

[10] H. Mozafari and A. Ayob. Effect of thickness variation on the mechanical buckling load in plates made of functionally graded materials. *Procedia Technology*, **1**, (2012), pp. 496–504.

[11] B. A. Samsam Shariat and M. R. Eslami. Buckling of thick functionally graded plates under mechanical and thermal loads. *Composite Structures*, **78**, (3), (2007), pp. 433–439.